Biochimica et Biophysica Acta, 936 (1988) 513–530
Elsevier

BBA 42903

Thylakoid volume, proton translocation and buffering capacity as measured with spin-label techniques

Bernd Wille

Institut für Chemische Pflanzenphysiologie der Universität Tübingen, Tübingen (F.R.G.)

(Received 21 April 1988)

Key words: Thylakoid; Proton translocation; Proton deposition; Amine distribution; Spin label; Kinetics

In model studies with lipid vesicles it is shown that the main population of the spin label Tempamine is bound to the membrane surfaces, the piperidine ring directed to the lipid phase. The signal of external label but not of label in the surface is broadened by chromium oxalate. Inner volumes of vesicles can be derived from the partially resolved polar part of the high-field line of Tempone or from the area of the Tempamine spectrum removed by making chromium oxalate enter the vesicles. If this membrane-associated population is corrected for, rotational correlation times for the label in the lumen can be obtained showing that hindrance of rotation is only by a factor of 3–5 instead of 10 as previously reported. In studies with thylakoids volumes of 1–3 μl/mg Chl were found with 0.3 M sorbitol as an osmoticum, 5 mM $MgCl_2$, 20 mM KCl, and 20 mM chromium oxalate. The internal buffering capacity and the magnitude of pH changes in the inner volume can be determined from flash-induced changes in the amine distribution. The buffering capacity is found to be 7–20 mM in buffer-permeable and approx. 100 mM in buffer-impermeable thylakoids, that is approx. 100 neq per mg Chl. The apparent H^+/e^--value in impermeable preparations was found to be up to 0.7 and lower in permeabilized material. ΔpH per flash is 0.04–0.06 units. Possible sources of errors, particularly the presence of non-functional or non-thylakoid membranes, are discussed. Time-resolved signals are presented and several side effects and their suppression are discussed. The response time of the method is up to 2 ms, protons from the donor side of Photosystem II can be separated kinetically from those liberated by the intersystem chain. While transients with less than 2 ms and approx. 20 ms were found with ferricyanide as an electron acceptor in accordance with the results with neutral red, pronounced slow phases ($t_{1/2}$ is several hundred ms) were found without acceptors. Evidence is presented indicating that at least part of these responses do not originate from the thylakoid inner volume.

Abbreviations: BSA, bovine serum albumin; Chl, chlorophyll; CP, 2,2,5,5-tetramethylpyrrolidine-3-carbonic acid-1-oxyl; chromium oxalate, potassiumtrisooxalatochromate(III); DBMIB, 2,5-dibromo-3-methyl-6-isopropyl-1,4-benzoquinone; DCMU, 3′-(3,4-dichlorophenyl)-1′,1′-dimethylurea; DCPIP, 2,6-dichlorophenolindophenol, sodium-salt; DML, dimyristoylphosphatidylcholine; DMQ, 2,6-dimethyl-*p*-benzoquinone; DMSO, dimethylsulfoxide; DPH, 1,6-diphenyl-1,3,5-hexatriene; DTA, 4-dimethylamino-2,2,6,6-tetramethylpiperidine-1-oxyl; FeCy, potassium hexacyanoferrate (III); FUV, french press unilamellar vesicles; HA, hydroxylaminehydrochloride; LA, *cis*-9-*cis*-12-octadecadienic acid, linoleic acid; LUV, large unilamellar vesicles; MV, methyl viologen; neutral red, 3-amino-7-dimethylamino-2-methylphenazine; PS, Photosystem; SUV, small unilamellar vesicles; TA, 4-amino-2,2,6,6-tetramethylpiperidine-1-oxyl; TN, 4-keto-2,2,6,6-tetramethylpiperidine-1-oxyl; TTA, 4-trimethylamino-2,2,6,6-tetramethylpiperidine-1-oxyl-bromide; Tes, 2-{[2-hydroxy-1,1-bis(hydroxymethyl)ethyl]amino}ethanesulphonic acid.

Correspondence: B. Wille, Institut für Immunologie, Domagkstr. 3, D-4400 Münster, F.R.G.

Introduction

In the recent discussion on the mechanism of the storage of energy for photophosphorylation, a salient point in the evaluation of chemiosmotic [1], microchemiosmotic [2], and more or less local [3,4] models of coupling of phosphorylation to electron transport rests on the determination of the magnitude of pH-changes inside organelles, internal buffering capacity, and the properties of the internal volume, An excellent review has been given by Ferguson [5]. A recent review of methods has been given by Kell [6].

While some indirect methods for pH measurement are available, direct measurement of proton deposition inside thylakoids depends essentially on the measurement of pH-indicating absorption changes of the membrane-bound amphiphilic dye neutral red [7,8]. The calibration of the neutral red response is indirect [9] and since its response to membrane potentials has been demonstrated in vesicle systems [10] the suspicion may arise that at least the quantitation of these results is biased. While it has been shown that the kinetics of proton efflux seen with neutral red in thylakoids coincide well with the response of dyes in the external medium [11], it may be worth while to establish an independent line of evidence for these phenomena. It has been shown that the distribution of the spin-labelled amine tempamine can be used to obtain similar information and a calibration of the response has been given [12]. Here data are scrutinized with respect to the location of tempamine as derived from the analysis of area and shape of spectra. The results are used to refine the calibration of flash-induced transients and to extend it to buffer-impermeable material.

The method is modified to accelerate the response to approx. 2 ms and time-resolved responses are presented.

The results presented here form part of a thesis by B. Wille.

Materials and Methods

Bovine serum albumin was from Sigma. It was excessively dialysed against standard buffer. DCMU was recrystallized from chloroform and washed with light petroleum. DMQ was recrystallized from ethanol/water. DTA was prepared by a variation of the procedure given in Ref. 13. 250 mg TN (1.47 mmol) were added to a solution of 1 g dimethylamine (29 mmol, recrystallized) and 0.11 g sodiumcyanoborohydride (17.6 mmol, Aldrich) and 2 g molecular sieve 3 Å in absence of methanol and stirred 96 h at 50 °C. The solution was filtrated, the solvent removed in vacuo, the product dissolved in water and extracted at pH 5 with chloroform. The product was extracted from the aqueous phase at pH > 9 with chloroform, and this procedure was repeated once. The main fraction obtained from a silica gel column (Merck Kieselgel 60, methanol, toluene 1 + 4) was dried over potassium carbonate and the solvent removed. The red oil crystallized slowly to yield 173.3 mg (60%) DTA. 14.03 N, 65.73 C, 12.36 H (8.88 O) $N_2C_{11}H_{24}O$ (calculated: $N_2C_{11}H_{23}O$) Fp: 50–51.5 °C, uncorrected. Other spin labels used were from Aldrich or molecular probes, purity was checked by TLC.

Soy-bean lecithin (Sigma, commercial grade) was ether-extracted according to Ref. 14, using light petroleum and acetone, a stock solution in hexane was kept at −18 °C under nitrogen for several weeks. The preparation of the other reagents used has been described [12].

Lipid vesicles were prepared according to Ref. 15 by sonication under nitrogen in a Bransonic R221 bath, the clear supernatant after 30 min or 1 h centrifugation at 100 000 × g used as small unilamellar vesicles (SUV). French press vesicles (FUV) were prepared according to Ref. 16 and large unilamellar vesicles (LUV) according to Ref. 17. Contrasting with 20% uranylacetate showed vesicle diamters of 16–225 nm (SUV) and 30–4000 nm (LUV).

DPH-labelled vesicles were obtained by mixing the stock solutions of lipids and DPH in a molar ratio of 1000 : 1 (assuming a molar weight of 750 for the lipids), evaporating the solvent, and shaking up in buffer. Sonication under nitrogen for 30 min produced a slightly turbid solution which was used directly.

Multilamellar lipid samples [18] were prepared by drying approx. 10 mg samples of DML (Sigma) in glass capillaries to constant weight over metallic sodium and adding the desired amounts of aqueous medium (with or without chromium oxalate).

After sealing under nitrogen, repeated heating in a glykol bath (approx. 120 °C) and mixing produced homogeneous samples and spectra which did not change on repetition of the mixing procedure.

Chloroplasts were prepared from market spinach (deveined leaves) or laboratory-grown peas (seedlings 2–3 week old) by grinding 50 g of plant material in 120 ml of 0.4 M sorbiol/20 mM Mes (pH 6.7)/0.5 mM $MgCl_2$/0.5 mM sodium isoascorbate/0.5 mg/ml polyvinylpyrroidone (25 000 D, phram. grade)/1 mg/ml BSA, for 5–10 s at high and 10 s at low speed in a commercial mixer. The pellet obtained after squeezing the juice through eight layers of cotton cloth and 2 min centrifugation at $2000 \times g$ was resuspended with a small brush in 0.3 M sorbitol/5 mM $MgCl_2$/20 mM KCl/0.2 mM Tes (pH 7.5) (hereafter referred to as buffer A). Debris was pelleted (20 s, 170 g), the chloroplasts sedimented as above and the pellet resuspended in 13 ml of 5 mM $MgCl_2$ and agitated gently for 1 min, the same volume of double strength buffer. A (but for $MgCl_2$) was added and the broken chloroplasts centrifuged down (4 min, $2000 \times g$). After a final wash in measuring buffer they were stored at 4–8 mg/ml Chl [19] in the dark on ice. Sometimes 30% of volume ethyleneglycol or 5% DMSO was added and the preparation stored under liquid nitrogen. To obtain intact chloroplasts [20], the first pellet of the above procedure was resuspended in 0.3 M sorbitol titrated to pH 6.7 with Tris base; the sediment after 15 s centrifugation at $2000 \times g$ contained chloroplasts usually more than 60% intact.

A preparation which produces buffer-permeable material has been described [12]. Intactness of the material was checked by phase-contrast microscopy [21] and the ratio of extinctions at 550 and 680 nm [22], and sometimes by the FeCy method [20].

PS II preparations were obtained by a modification of the method of Ford and Evans [23], using a medium of 15 mM NaCl, 5 mM $MgCl_2$, 2 mM Mes (pH 6.3) for incubation and resuspension. The results reported here could be reproduced with the methods given in Ref. 24, and the MDT treatment of [25] as well as the original procedure by Berthold et al. [26].

ESR measurements were performed at a Varian E-Line Century spectrometer interfaced to a Bruker Aspect ER140 data system. For kinetic measurements a Varian E 238 (T_{110}) cavity and flat cells were used. The signal channel was replaced by an EG&G HR 8 lock-in amplifier. The system was operated at 25 kHz modulation and permitted response times of 100 μs or more.

Volume determinations were done using a rectangular cavity and heat sealed 0.8 mm (internal diameter) glass capillaries in 3 mm capillaries. Flash illumination was provided by a General radio Strobotac with auxiliary capacitance (8 μs at 1/3 height) through a lens or a 1000×10 mm light guide and a Schott KG 3 heat filter. When used with the lens, the flash produced a small 'spike' of changing polarity and approx. 3 ms duration. This artifact was not suppressed when only slow responses were to be monitored to keep the number of accumulations small. pH was measured in 200 μl samples with small pH-electrodes (Metrohm, Ingold) frequently cleaned mechanically and with pepsin/HCl, using 1 M KCl as internal electrolyte.

Difference spectra were obtained by optimizing the subtraction factor for an optimal baseline (the essentials are given in Ref. 27). Buffering capacities were estimated with glass-electrodes in a thermostated vessel from the pH changes (up to 0.05 pH) induced by μl addition of calibrated HCl.

Weakly buffered samples were titrated to the desired pH prior to measurement. Since the equilibration of the sample with the ESR-cell surface caused a pH-shift of approx. −0.2 units, the pH referred to is measured after redrawing the sample from the cell.

Timing of data acquisition, data manipulation and nonlinear least-squares analysis [28] were performed on a Bruker ER 140 data system. Calculations (disregarding the back reaction) usually produced stable fits with three phases and signal-to-noise ratios of at least 15, which, however, does not indicate a true resolution of phases unless additional evidence can be obtained.

Simulations of kinetics were done either using analytic expressions for simple proton transport with back diffusion or by Runge-Kutta simulations [29] of the 4th order.

Photosynthetic units are expressed as the number of Chl per 0.25 O_2 evolved per flash as mea-

sured from trains of 40–80 flashes of the flashlamp at saturating intensity in a Yellow Springs oxygen electrode thermostated at 20 °C, buffer A usually supplemented with 5 mM Tes (pH 7.5), and 5 mM FeCy or 0.5 mM DMQ as electron acceptors, 10 μg/ml Chl.

Correction of fluorescence for trivial absorption was performed using extinction coefficients of the spin-labels at different wavelengths determined in the vesicle suspension. The fluorescence spectra were obtained in a Yobin Yvon JY 3D Spectrometer interfaced to a HP 9815 computer and plotter. The real quench was calculated from $Q = 1 - 10^{q}$ and $q = (E_1 - E_2\varepsilon^*)/(1 - \varepsilon^*)$ with $\varepsilon^* = (\varepsilon_2 + \varepsilon_{ex})/(\varepsilon_1 + \varepsilon_{ex})$, the indices em, 1, 2 referring to emission, and ex to excitation wavelengths. From simple geometric considerations it follows that $\varepsilon_{app} = (\varepsilon_{em} + \varepsilon_{ex})/2$ and $E_{1,2} = q + a\varepsilon_{app}d$, which was a good description of the empirical values. Actually, the ε_{app} values for 2–4 mM spin-label were used to correct all the data, above and below these values the resolution was not sufficient. The procedure resulted in linear Stern-Vollmer plots.

Results

Location of the probe in model systems

Several studies have been carried out to study the location of spin-labels in model systems like vesicles [18] and to examine binding to thylakoid membranes [30,31]. The issue was reexamined under the experimental conditions of this study.

Fig. 1 shows the results with samples of multilamellar lipids: there is a marked change in anisotropy of TA between spectra above and below the transition temperature and the addition of chromium oxalate during sample preparation reveals a lipid-bound population inaccessible to broadening and almost independent of the lipid/water ratio. The changes in the spectra with temperature are easily understood as the superposition of a similar population, changing the shape of its spectrum with the fluidity of the membrane, and a small signal from a population rotating quickly and isotropically.

Unilamellar vesicles produced composite spectra after correction for insufficiently broadened external signal [27], the narrow contribution to the

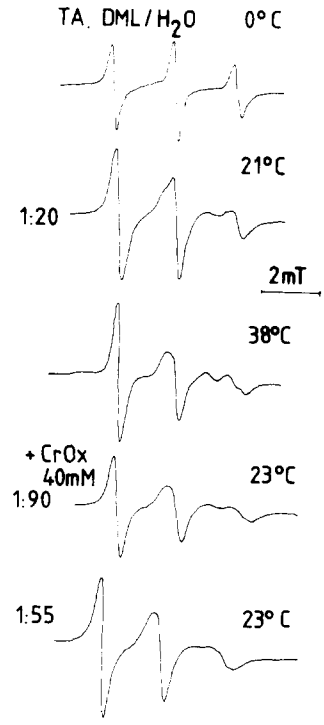

Fig. 1. Spectra of TA in multilamellar lipids, effect of temperature. DML; preparation, see methods; numbers give ratios DML/H_2O; modulation, 63 μT; microwave power, 20 mW; retraced. 1 mM TA/TO, samples with chromium oxalate: 20 mM TA (1 : 90), 0.8 mM TA (1 : 55) 40 mM chromium oxalate.

lines was increasing with vesicle size. In small vesicles, the signal of TTA (Fig. 2), a label assumed not to enter the inner volume [30,32] was very similar to that of TA, its area sharply decreasing with temperature. Tempamine spectra below 12 °C are closely resembling spectra of a homogeneous population of spins undergoing isotropic rotation, but changes with temperature of the anisotropy of the signal are similar to those seen in Fig. 1 and the signal from the impermeable label TTA indicates that the situation is more complex: there is obviously a population of spins inaccessible to chromium oxalate at the outer surface of the vesicles.

In chloroplasts, pronounced changes are seen in the spectra directly after mixing. They are attributed to diffusion of chromium oxalate into the stroma and some damaged thylakoids, osmotic responses and the entry of potassium into the thylakoids. They are much smaller or absent with

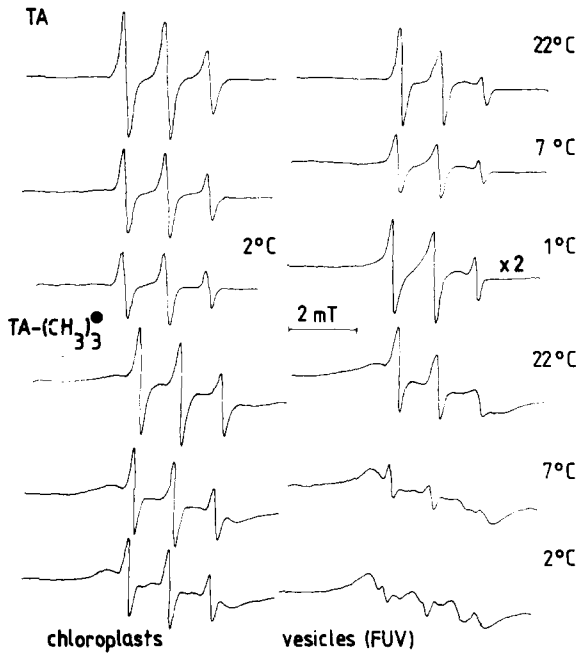

Fig. 2. Difference spectra of TA and TTA in chloroplasts and FUV, Effect of temperature. FUV ≈ 24 mg/ml, chloroplasts (lettuce) 4.7 mg/ml Chl, 0.3 M sorbitol, 20 mM KCl, 5 mM $MgCl_2$, 5 mM Tricine (pH 7.5), 20 mM chromium oxalate, 1.2 mM TA/TTA, spectra on one sample starting at 22°C, the effect is reversible. Microwave power, 40 mW; modulation, 63 μT.

TTA. A constant shape of the spectra was usually found after about 10 min. Rotational correlation times were calculated from line heights [33] because it was found that more sophisticated methods [34,35] cannot be applied to signals of tempamine, whose hyperfine splittings depend on pH and polarity of the medium (Wille, B, unpublished results). In intact material the rotational correlation times were more than $4 \cdot 10^{-10}$ s, the anisotropy (expressed as ε according to Ref. 36) was approx. -0.2. τ and ε are only handy descriptions of spectral shapes, since the spectra used are obviously composite signals.

To calculate volume ratios from these spectra double integration should be used, a method prone to serious errors in the presence of small amounts of unresolved and/or incorrectly subtracted external signal in the baseline. Therefore the formula $A = p\Delta W^2 I$ is preferred (A, area; Δ/W, first derivative peak-to-peak width; I, height of central line), where p is a factor that depends on the gaussian contribution to line shape [34] and it was checked that errors introduced are less than 30% (underestimation) of the lines of more slowly moving nitroxide by comparison to that in water (model studies in saccharose solutions and integrations of spectra simulated with the hyperfine splittings given in Ref. 35).

If TN was used the negative highfield peak (taken as $1/2I$) and the width of the central line (see below) could be used as a rough approximation. TN and CP produce with broken chloroplasts surprisingly small values (up to 16% of the figure with TA) and TTA results (up to 87%) close to those found with TA. Attempts to make chromium oxalate enter the thylakoids by sonification (2–4 min at 20°C, bath) or with the ionophore Alamethicin [37] remove from the spectra a population with the spectrum shown in Fig. 3c and d. The volumes calculated from these signals with TA coincide within a factor of about 2 with those found with TN, where the same treatments remove virtually all the polar component of the spectrum (Fig. 3). With TN the width of the polar high-field line is almost identical to that of the center line at the (limited) experimental precision, justifying the above approximation. For a more sophisticated technique not feasible with our small signals (see Ref. 38). Table I gives the results obtained with different techniques. Usually the use of TN, CP or permeabilization results in coinciding figures for the internal volume, taken here as the correct estimate, whereas TA produces an overestimation due to the membrane-associated population already deduced from the TTA spectra. Similar results seen with CP and TN argue against a major contribution of Donnan potentials (as can be expected with 20–40 mM chromium oxalate which means 60–120 mM K^+ in the buffer).

Due to the small internal volume the difference spectra are not very precise, in addition they may contain contributions due to changes in the state of membrane lipids during permeabilisation. Preliminary estimates of the apparent rotational correlation times in the signals obtained are $1.2 \cdot 10^{-10}$ s to $1.7 \cdot 10^{-10}$ s for the signal of TA (compared to $6.4 \cdot 10^{-10}$ s for the total signal and $4 \cdot 10^{-11}$ s in 0.3 M sucrose), and $6 \cdot 10^{-11}$ s to $7 \cdot 10^{-11}$ s for TN ($1.4 \cdot 10^{-11}$ s in 0.3 M sucrose). It follows a

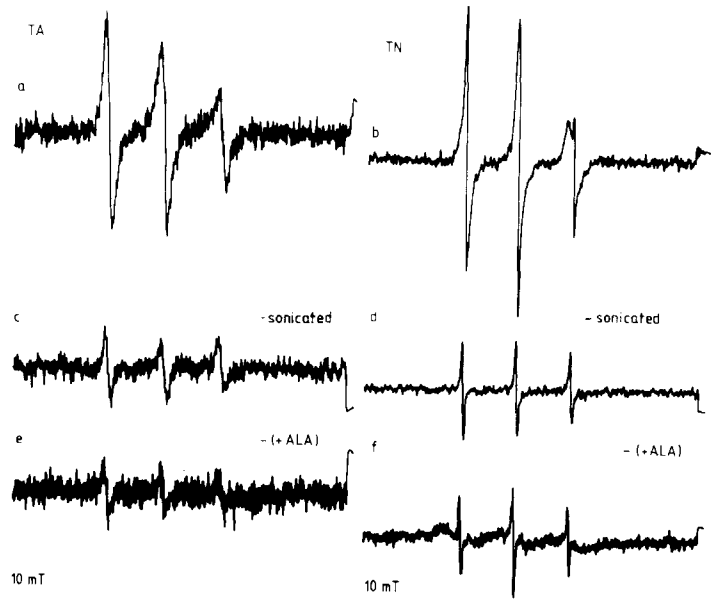

Fig. 3. Spectra of TA and TN in chloroplasts, permeabilization of chromium oxalate. (a) TA; (b) after subtraction of a sample without chloroplasts; (c) TA, after subtraction of a sample sonicated 4 min (see text); (d) TN, as (c); (e) TA, after subtraction of a sample with Alamethicin 130 nmol/mg Chl; (f) TN, as (e). The spectra shown may contain residual signals due to changes in membrane structure. 0.3 M sorbitol, 20 mM KCl, 5 mM $MgCl_2$, 5 mM TES (pH 7.75). 20 mM chromium oxalate, 1.5 mM TA, TN 3.1 mg/ml chloroplasts, four spectra accumulated, 2 min/10 mT. Time constant, 30 ms; microwave power, 20 mW; modulation, 8.3 μT.

TABLE I

COMPARISON OF SPECIFIC VOLUMES OBTAINED BY DIFFERENT METHODS

Sample	[Chromium oxalate] (mM)	V^* (μl/mg Chl)			Factor V^*_{TA}/V^*_{TN}
		TA	TN [f]	Permeabilized	
Lettuce, fresh	20	16	2.45	–	6.5
Lettuce, fresh	40	3.8	0.6	0.9 [b]	6.5 4.5 [g]
Lettuce, fresh	40	10.4 ± 0.9	0.7 ± 0.06	–	14.6
Spinach, fresh	20	20	6.3	3.2 [c]/3.8 [b] 1.3 [d]/2.4 [e]	5–6 [g] 8–15 [g]
Peas, fresh	20	21.5 ± 3.5	1.5	–	13.8
Peas, fresh	20	16.6 ± 2	–	5.6	
Lettuce, N_2 [a]	20	17.5 ± 1.4	1.4 ± 0.3	–	11.8
Spinach, N_2 [a]	20	17.8 ± 3	1.4 ± 0.1	–	12.7
Peas, N_2 [a]	20	15.8 ± 1.5	–	3.3 [d]	4.7
Peas, N_2 [a]	20	5.7 ± 0.7	0.8 ± 0.07	–	7.3

[a] Stored under liquid nitrogen with 33% ethyleneglycol.
[b] From difference spectrum ± sonication, TN.
[c] From difference spectrum ± sonication, TA.
[d] From difference spectrum ± alamethicin, TA.
[e] From difference spectrum ± alamethicin, TN.
[f] From approximation for high-field line, TN (see text).
[g] Values refer to chromium oxalate-permeabilized samples.

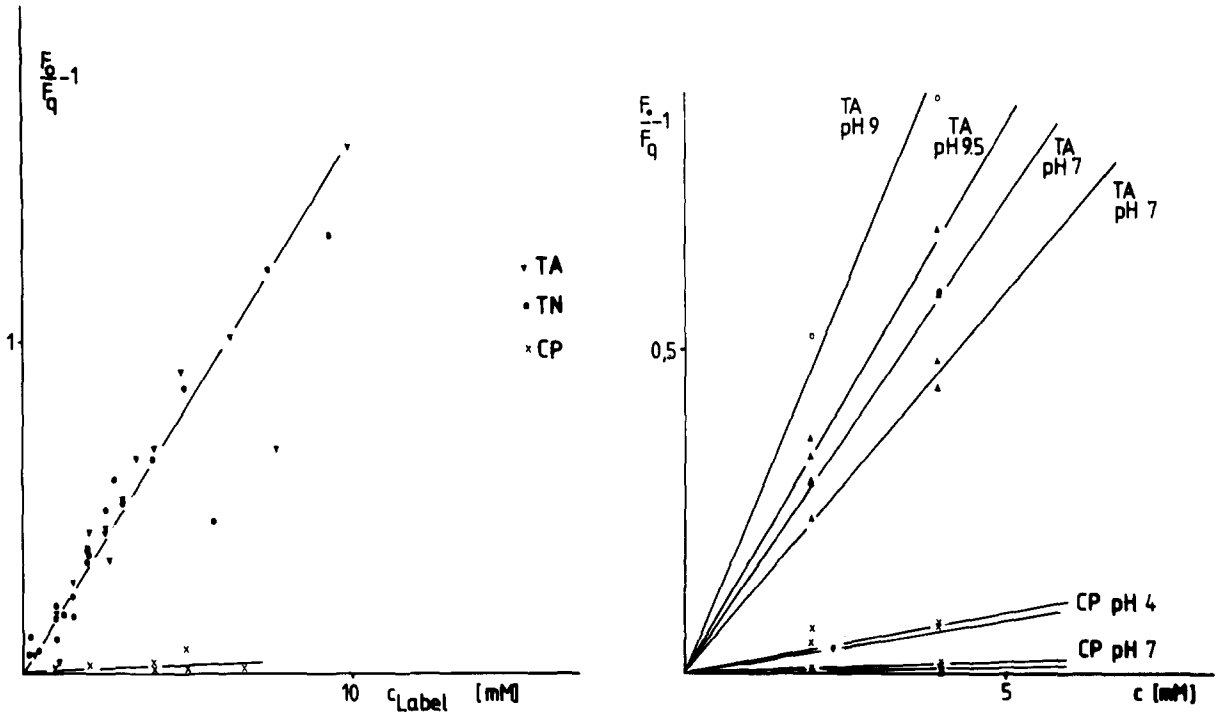

Fig. 4. Stern-Vollmer plots of quench of DPH-fluorescence at (a) 430/470 nm (TA/TN), or 410/490 nm (CP), excitation 330 nm. 15 mM NaCl, Tricine 5 mM (pH 7.5) + DPH-vesicles 0.85 mg/ml lipid. (b), as (a), but CP measured at 410/450 nm, 0.22 mg/ml lipid, 50 mM potassium phosphate (pH 7), 50 mM potassium citrate (pH 4), or 50 mM sodium borate pH 9 or 9.5. Results from two different preparations of vesicles, Prep. 1: open/closed circles (TA), crosses (CP); Prep. 2: open/closed triangles (TA), triangles (CP).

hindrance in rotation of a factor 3–5 instead of the factor 10 derived from the total signal [27].

For technical reasons it was not yet possible to obtain spectra of illuminated samples [39].

Independent evidence for the location of a population of spins at the membrane surface

Vesicles prepared from soybean lecithin were labelled with DPH, which is believed to be located exclusively in the membrane lipid phase [40]. Addition of nitroxides caused a fluorescence quench, which (when corrected for trivial absorption) produced linear Stern-Vollmer plots. Fig. 4a shows that TA was nearly as efficient as TN, whereas CP produced only a small (if any) quench at pH 7.5. When charged and uncharged forms of the labels were compared, titrating CP-samples to pH 4 produced at least a 2-fold increase of efficiency, whereas TA at pH 9–9.5 was only 30% more efficient than at pH 7.5 (Fig. 4b). TTA (not shown) was slightly less efficient than TA at pH 7.5. It follows that the interaction of charged amine labels with the membrane interior is more pronounced than would be expected if the nitroxide group was directed to the water phase.

Calibration of flash-induced amine redistribution in thylakoids

Details of the procedure are given in Ref. 12. The response of the charged amine to membrane potentials can be tested by the addition of valinomycin, which was found not to change the amplitude of the signals. The response is sensitive to DCMU and decouplers [12]. The derivation given in the Appendix relates the proton-to-electron ratio p to $\Delta I/I$ (relative change in line height) according to

$$p = r\frac{N}{C}\frac{\beta_1}{\ln 10}V'(K+h_e)\frac{\Delta I}{I}\frac{(1+g'V')}{(1+g\beta'V')} = \frac{\beta_i}{\ln 10}p_b$$

(r correction for nonlinearity of response [12], β

buffering capacity, C chlorophyll concentration; N, photosynthetic unit; V', β', ratios of internal to external buffering capacities and volumes; g, g', see below). Several correction factors have to be included to account for experimental errors. g: accumulation of TA in the aqueous internal volume, obtained from the data in Table I, comparing values found with TA by making chromium oxalate leak into the inner volume and with TN (less than 2, probably near unity). g': total accumulation of TA in aqueous and membrane environments, comparing volumes from TN and TA (total signal) in Table I (5–15, see righthand column). g_1: error in volume estimation due to accumulation of spin label ($=1$ for volumes estimated with TN; $=g'$ if total TA signal is used). g_2: change in buffer capacity due to accumulation of (cationic) buffer or amine, from accumulation of tempamine and comparison of different buffers (this factor is equal to g' for TA and near unity for permeable zwitterionic buffers used – see below). Photosynthetic units of 265–300 Chl (the latter value used in calculations) were found for the pea chloroplasts used in these experiments. While this is clearly an underestimation due to the double hits produced by the long flash used, it is the functional value for this study.

Two procedures are feasible; using buffer-permeable thylakoids [9,12] a plot according to (the subscript app denoting uncorrected experimental values)

$$P_{\mathrm{b\,app}} = \frac{N}{C} V'_{\mathrm{app}} \frac{\Delta I}{I(K+H)}$$

and

$$\frac{1}{P_{\mathrm{b\,app}}} = \frac{\beta_{\mathrm{int\,app}}}{p \ln 10} + \beta_{\mathrm{b}} + \frac{\beta_{\mathrm{TA}}}{p \ln 10}$$

may be used to obtain β_{int} and p, the proton-to-electron ratio. Fig. 5 shows the results of such an experiment with several buffers and chloroplasts prepared according to Ref. 12 and stored under liquid nitrogen in presence of 5% DMSO.

Inserting the corrections produces for buffers entering the thylakoids $p_{\mathrm{app}} = g_1/gg_2\,p$ and $\beta_{\mathrm{int\,app}} = \beta_{\mathrm{int}}/g_2$. With $g_2 \approx 1$ from the apparent equal efficiency of different buffers and, consequently,

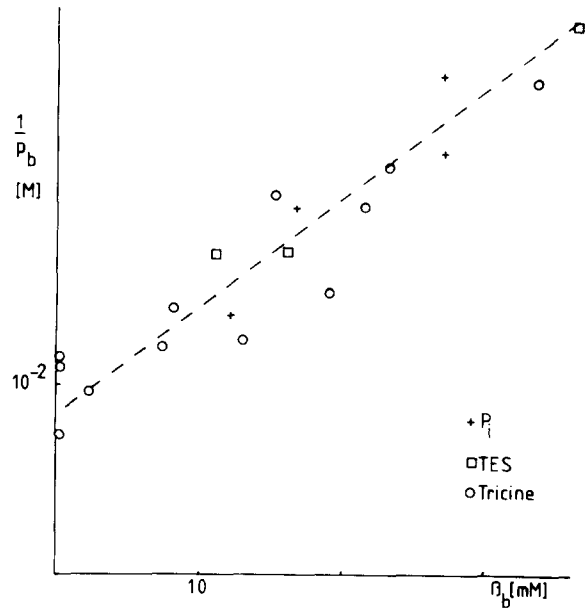

Fig. 5. Plot of p_{b}^{-1} against concentration of permeable buffers (see appendix). Pea chloroplasts 2.9 mg/ml, stored under liquid nitrogen in the presence of 5% DMSO, 5 mM TA, 40 mM chromium oxalate, 0.1 M saccharose, 20 mM KCl, 3 mM $MgCl_2$; microwave power, 80 mW; modulation, 25 μT.

$g \approx 1$ and $g_1 \leq 10$ (volumes derived from uncorrected TA-spectra at 0.1 M saccharose) and using volume data derived from TA corrected with g_1 we get $\beta_{\mathrm{int}} \approx 2$–$20$ mM, and $p < 1$ ($\beta_{\mathrm{int\,app}} = 15$ mM, $p_{\mathrm{app}} = 0.8$; typical uncorrected data range from $\beta_{\mathrm{int\,app}} = 2$–$20$ mM and $p = 0.5$–3).

In freshly and quickly prepared material, almost no buffer effect was visible and a second method was used based on the term $(1 + g\beta' V')$ approaching unity when $\beta' \leq 10$ due to addition of external buffer if $g \leq 2$ (volume data). Thus we obtain

$$\beta_{\mathrm{int\,app}} = \left(\frac{p_{\mathrm{b\,app}}}{p_{\mathrm{b\,app^b}}} - 1 \right) \frac{\beta_{\mathrm{b}}}{gV'_{\mathrm{app}}} - g_2 \beta^*_{\mathrm{TA}}$$

($p_{\mathrm{b\,eff^b}}$: in the presence of small amounts of buffer $1 + gV'\beta' \approx 1$).

β_{b}, the external buffering capacity is obtained from the response of a glass electrode in a concentrated suspension of thylakoids at 4° C. It can be resolved in quick responses and the slow response expected from leakage of protons into the internal volume [41] (the expected time course can

TABLE II

CALCULATION OF BUFFERING CAPACITIES AND H^+/e^--VALUES FROM $\Delta I/I$ VALUES

Samples: buffer A 20 mM chromium oxalate, 0.4 mT modulation, power 100 mW, ten events accumulated, sample incubated more than 10 min, buffer added immediately before measurement. Volumes used in calculation from TN-spectra or values with TA/10. Diminution of $\Delta I/I$ by impermeable buffers in pea chloroplasts (see appendix for definition of the terms used, given: mean and standard deviation, $n = 2$–3).

Expt.	pH	$[c_{TA}]$ (mM)	[Chl] (mg/ml)	Buffer	V'/[Chl] (μg/ml)	$\Delta I/I$ ($\times 10^2$)	$[\beta_b]$ (mM)	$(p^u_{eff}/p^b_{eff})^{-1}$	$[\beta_{iapp}(TN)]$ ** (mM)	p_{app}
1 *	7.7	1	2	Tes	9.18	0.264 ± 0.04	0.74			
						0.175 ± 0.01	6.5	0.51	189	0.08
2	7.5	2	2.17	Tes	8.12	2.31 ± 0.29	0.88			
	−7.75				0.72 (TN)	2.0	14.45	0.16	90.1	0.32
			1.55			2.73 ± 0.21	0.7			
						1.97 ± 0.04	14.45	0.38	238	0.86
						2.31 ± 0.1	41.7	0.18	112	0.48
			0.78			1.95 ± 0.24	0.51			
						1.76 ± 0.35	16.8	0.11	100	0.32
3	7.6	2	1.36	Tes,	11.6	2.24 ± 0.15	0.70			
	−7.8			Tricine		1.76 ± 0.21	27.9	0.27	138	0.60
						1.75 ± 0.04	98.1	0.28	139	0.62
			0.68			1.46 ± 0.2	0.53			
						1.44 ± 0.19	27.7	–	–	–
			0.34			0.94 ± 0.05	0.45			
						0.91 ± 0.18	27.6	–	–	–
4 *	7.5	1	1.66	Tes	20.4	7.6 ± 0.02	0.62			
					1.55 (TN)	7.76 ± 1.1 ***	0.62			
						6.8 ± 0.46	14.2	0.12	28.7	0.74
						7.35 ± 0.78	27.8	0.03	–	–

* No effect at lower Chl concentrations.

** Buffering capacity of TA and buffer ≤ 0.36 mM.

*** +25 mM KCl.

be obtained from the decay of the response after illumination). The slow response was very small and insensitive to Gramicidin, which may indicate that this part of the signal is an artefact. Leaving the assessment of this response open, we may, nethertheless estimate an external buffering capacity of no greater than 0.25 μEq/mg Chl from the fast phase, which compares quite well with data from the literature (0.3–2.4 μeq/mg Chl [42,43]) for the total buffering capacity.

BSA, the most popular impermeable buffer [9], was found to stimulate the signals from several of our preparations, an effect which could be reproduced with O_2 evolution under flashing light and is most probably due to reversal of inhibition of part of the preparations with fatty acids [44,45]. Table II shows that the experiment can also be done with small hydrophilic buffers. Two extreme examples (1, 4) and two typical ones are displayed. In most of our experiments the buffering effect was below experimental precision, the buffering capacities given are thus to be considered as upper limits.

This type of experiment produces $\beta_{int\,app} = g/g_1$ β_{int} and $p_{app} = p$ and we get $\beta_{int} \approx 100$ mM, i.e., ≈ 100 neq per mg (in experiment II) and $p \approx 0.7$ for the experiments II and III with $g_1 = 1$ (for TN) and $g < 2$ (Table I) (uncorrected $\beta_{int\,app} \approx 100$ mM and $p_{app} \approx 0.4$–0.8 assuming $g = 1$). Note that the value of p is obtained without any corrections here.

An additional problem which cannot be solved yet can be inferred from the spectra with TTA: the relative high values of volumes obtained with

TTA do not correspond to only about 50% of the surface being accessible to the label as expected with thylakoids. It can thus not be excluded that a considerable amount of membranes in the preparations do not represent functional thylakoids (outer membranes, etc.). This will lead to an overestimation of I and, consequently, to an underestimation of p in both types of experiments.

ΔpH

No volume estimation interferes and thus only the aforementioned ambiguity and problems due to TA enrichments affect this parameter, which was found $\Delta pH \leq 0.04$–0.06 at pH 7.5–7.8, increasing by a factor approx. 2 when the pH is shifted to 7.2 (a deviation from the dependence on pH reported by of other authors [9] which has not yet found an explanation).

Kinetics of proton deposition under single turnover flashes as measured with TA.

Response to proton transport

The apparent half time of the fastest phase of proton transport detected with tempamine was more than 30 ms at pH 7 and decreased with pH, reaching values of 2–5 ms still higher than the of 1 ms or more half-time expected [46] near pH 8. Increasing TA concentrations (2–5 mM) accelerated the response, while at high pH and TA or after excessive illumination the fast rise was lost and a half-time of about 20 ms was found. Inhibition of the oxygen-evolving system takes place under these conditions (Ref. 47, checked by measuring steady-state oxygen evolution). A change of pK of the amine used (DTA, p$K \approx 8.6$ under the conditions used) produced an accelerated response: apparent half-times of approx. 2 ms were found even at 0.6 mM DTA and pH 7.5. Fig. 6 shows the transient obtained at high time resolution. A small delay of the quick rise was found which was somewhat variable (200–600 μs) and is at the limit of resolution of our present instrumentation. Simulations of the amine distribution across a membrane, using a Runge-Kutta procedure produced a similar lag when the diffusion of amine across the membrane was made rate-limiting.

Side effects

In an experiment designed to test for contributions of residual external signal and spin label reduction in the light to the kinetics, the shape of the kinetics was virtually unchanged when the amount of the external signal was varied by a factor of more than 5 by changing the concentration of chromium oxalate from 10 to 40 mM.

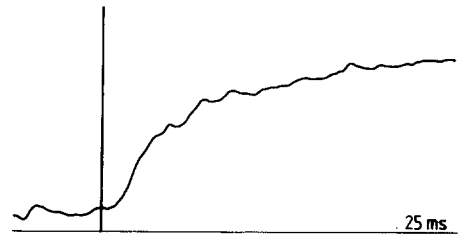

Fig. 6. Rapid phase of transient on TA-line. 0.3 M sorbitol, 20 mM KCl, 5 mM $MgCl_2$, 0.2 mM Tes (pH 7.5–7.8), 0.83 mg/ml Chl, 15 mg/ml BSA, 0.6 mM DTA, 20 mM chromium oxalate; modulation, 0.26 mT; microwaves 100 mW; light guide and filter, flashes 1 Hz; time constant, 100 μs; two samples, 400× each. The line gives the position of the trigger impulse (see text).

Slow kinetic phases of proton deposition

We denote by 'slow' half-times surpassing 20 ms. Fig. 7 shows that the amount of this response was considerable. Since the half-time of the back reaction is more than 20 s, in accumulations some building up of ΔpH cannot be avoided and there is some interference of the back reaction with these slow esponses.

Methyl viologen did not change the kinetics observed, but FeCy produced above about 1 mM the well-known [7] 20 ms response as the only slower component (Fig. 7c). The signal without FeCy was used for calibration because of the better signal-to-noise ratios. $\Delta I/I$ ratios were similar or even higher with FeCy, but obviously part of the preparation was permeable to this substance at least on a minutes timescale [27]. FeCy broadens nitroxide lines and consequently leads to smaller and time-dependent responses.

DBMIB left only the fast response at 300 nmol/mg Chl, this inhibition worked also without FeCy but then on the midfield peak of the nitroxide spectrum the kinetics were distorted due to transients from semiquinone signals.

The slow responses were not suppressed by reduced osmolarity (Fig. 7b), storage under liquid nitrogen in the presence of 5% DMSO (Fig. 7e),

nonpermeant buffers (not shown) or moderate amounts of valinomycin (Fig. 7f) (at 25 μM, which would be equivalent to 150 nM at 10 μg/ml Chl). High amounts of this K^+-ionophore accelerated the decay of the signal and obscured the effect.

The amount of slow phase varied in the preparations tested. Similar to slow phases reported by Hope and Matthews with the neutral red technique [48], it could be demonstrated with firmly stacked and partly unstacked preparations (in the absence of $MgCl_2$ and with only 10 mM chromium oxalate, data not shown) and was reduced

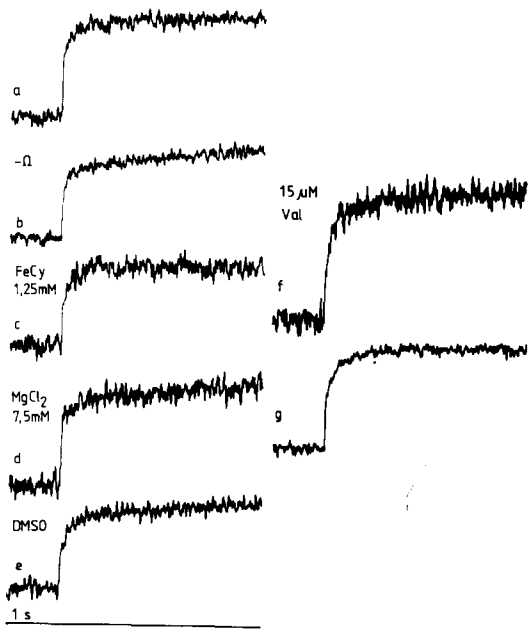

Fig. 7. Slow phases of flash-induced transients on TA-lines. 0.3 M sorbitol, 20 mM KCl, 5 mM $MgCl_2$, 63 mM Tes (pH 7.5), 0.98 mg/ml Chl, 1.2 mM DTA, 20 mM chromium oxalate, 12.5 mg/ml BSA; flashes 0.25 Hz; time constant, 1 ms, 0.41 mT; 100 mW. The results of computer fits are given for the kinetics (half-time of response and contribution to total response) allowance was made for three phases, which generally produced better fits than two phases only, precision of the parameters for the intermediate phase is usually limited. (a) fit: 2/16/48 ms, 61/20/18%; (b) 0.15 M sorbitol, 1/8/243 ms, 25/44/29%; (c) 1.25 mM FeCy 4/22 ms, 40/60%; (d) 0.15 M sorbitol, 7.5 mM $MgCl_2$, 2/19/25 ms, 76/9/14%; (e) stored under liquid nitrogen with 5% DMSO, 0.5 mM TA, 1.18 mg/ml Chl, 25 mM Tes (pH 7.5), 2/14/1407 ms, 23/25/51%; (f) 0.3 M sorbitol, 20 mM KCl, 5 mM $MgCl_2$, 0.2 mM Tes, 15 mg/ml BSA (pH 7.45), 0.6 mM DTA, 20 mM chromium oxalate; 1 mg/ml Chl (lettuce), 25 μM valinomycin, 10/105 ms, 70/30%; (g) control, 5/43 ms, 54/45%.

Fig. 8. Effect of uncouplers on flash-induced transient on TA-spectrum (low-field line), simulation of decay kinetics. 0.3 m sorbitol, 20 mM KCl, 5 mM $MgCl_2$, 12.5 mM Tes (pH 7.5), 0.8 mg/ml Chl, 0.35 mM DTA, 20 mM 12.5 μM gramicine D, 1 Hz. 84×, time constant, 100 μs; modulation 0.26 mT; microwaves, 100 mW. Computer simulations included (fit 1 shifted for clarity): Fit 1: back reaction $t_{1/2}$, 1.5 s; rise time, 1/20 ms; 50/50%. Fit 2: back reaction $t_{1/2}$ 1.5 s; rise time, 1/20/100 ms, 40/30/30%. Fit 3: back reaction $t_{1/2}$, 1.5 s, rise time 1/20/120 ms, 40/40/20%.

by preillumination. The slow responses showed a pronounced time dependence, decreasing with incubation time under otherwise unchanged conditions.

A stimulation of the reaction is seen after a short (5–10 min) incuation with linoleic acid, diminishing or (most likely) being obscured later by an increase of membrane permeability for protons. Concentrations exceeding the 50–100 μM linoleic acid needed to produce this effect result in membrane damage and inhibition of electron transport [49].

In part of the preparations used the reaction in question was more contrasted on the high- than on the low-field line (not shown).

Fig. 8 shows the response of the slow phases to uncouplers. When gramicidin or nigericin were added at concentrations which led to half-times of the decay in the range of 1–2 s, the resulting responses could be nicely fitted by assuming a

50%/50%, 1/20 ms rise and a decay read from a slow scan at more than 2 s after the flash (fit 1), while the assumption of slow phases even of smaller amplitude than in the control samples led to considerable deviations from the experimental results (fits 2 and 3).

Dark-adapted sampled showed no oscillations with period 2 in the slow phase (eight flashes, 1 Hz, not shown).

Effect of deactivation of Photosystem II

If PS II was inhibited at the donor side by alkaline pH or treatment with 100 mM HA [50], the signal after a flash declined below the baseline at alkaline pH. Apparently, a negative transient is superimposed on the signal from residual proton transport. A response with the same kinetic characteristics and insensitivity to uncouplers (see below) could be demonstrated in as simple a system as PS II-enriched membrane preparations.

Difference spectra of these membrane preparations show a small, virtually isotropic signal of a chromium oxalate inaccessible population which is very sensitive to changes in $MgCl_2$ and chromium oxalate concentration (decay from $V^* \approx 4$ μl per mg Chl to $V^* < 1$ μl per mg Chl when changing from 0.1 or less to 5 mM $MgCl_2$).

The flash-induced signal on the low-field line of the TA spectrum (Fig. 9) was found sensitive to very small concentrations of hydrophilic buffers. Uncouplers suppressed the signal only at extremely high concentrations (not shown).

The response was suppressed by DCMU and stimulated by electronn acceptors like DMQ (0.5 mM), whereas FeCy stimulated at low (below 1 mM) and suppressed at higher (over 5 mM) concentrations. At flash frequencies above 0.3 Hz, the signal saturated quickly.

The effect with DTA and TA produced very similar responses to pH (a pronounced decrease below pH 7.8 and irreversible effects below pH 7.5 where a preincubation at pH 9 – i.e., alkaline inactivation of PS II by the spin-label amine present – led to an increase of response) inspite of the change in amine pK, whereas it was not possible to demonstrate the reaction with TTA. The data shown contain a minor contribution due to a simple thermal effect in unbuffered media, which led to a decrease of signal upon illumination and

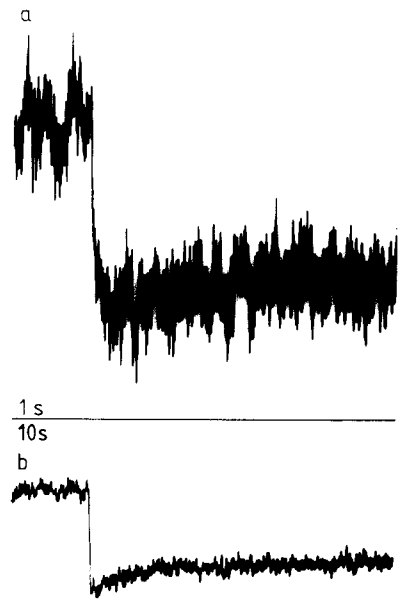

Fig. 9. Flash-induced signal on PS II-enriched preparation accordingto Ref. 11. Modulation, 0.26 mT; microwave power, 100 mW; 3 mM TA, 20 mM chromium oxalate. (a) 0.3 M sorbitol, 20 mM KCl, 30 mM $MgCl_2$, 0.2 mM Tes 0.5 mM DMQ (pH 7.6), 0.47 mg/ml Chl, 15 mg/ml BSA; approx. 200×, time constant, 1 ms. (b) 0.3 M sorbitol, 0.2 mM Tes, 0.67 mg/ml Chl, time constant, 10 ms; (pH 7.8).

can be obtained in chromium oxalate solutions with TA alone.

Discussion

Dynamics of small nitroxide labels have been studied in detail by Keith et al. [18] who found that uncharged labels like TN show signals from nonpolar and polar environments. The lines from membrane interior seems to disappear due to hindrance of rotation below the phase transition, whereas the partition coefficient (from the areas) rests virtually unchanged. Tempophosphate and CP showed marked changes in the anisotropy and rotational correlation time at the transition temperature, whereas TA did not when assayed in the charged form (below pH ≈ 9). It was concluded that TA was located near the surface of the membrane, the ring directed towards the aqueous medium.

The conclusions concerning the location of tempamine at the membrane surface to be drawn

from the results of this study are obviously at variance with these notions. Spectra obtained from the internal volume of vesicles or organelles with TA at 12–15°C can very easily be mistaken for signals indicating quick, isotropic rotation. This would be even more probable if membranes used in other studies [31,32] were more rigid at the measuring temperatures. There is a simple test for mixed signals that can be performed under conditions: areas of the spectra calculated for all three lines should be equal within the limits discussed above (the shape is predominantly gaussian). With our mixed signals from tempamine, however, the area is always much smaller when calculated from the high-field than from the mid-field line, a phenomenon which seems to be present also in the spectra reported by other workers ([39] Fig. 1).

The observation of Keith et al. [18] of only slightly changed hyperfine splittings and motion parameters at the phase transition of the membrane is easily understood if the dimensions of the molecules involved are considered: TA with its charged group residing close to negatively charged lipid headgroups will, when directed to the membrane interior, 'see' with its nitroxide group only the region of C_3–C_4 of the lipid side chains which is known to be ordered and rather polar, both parameters are likely to undergo smaller changes upon 'melting' of the hydrocarbon part of the membrane than motional parameters measured in the center of the membrane. Such an orientation would explain anisotropy of rotation (the rotation being around the N–O bond, see Ref. 51), hindrance of rotation, an environment rather polar and not very susceptible to changes in lipid order, a shielding against chromium oxide, and easy interaction even of the charged amine with DPH.

Binding of TA to thylakoid membranes was examined [30,31] and it was shown that enrichment of the label in pellets of chloroplasts was negligible and the amine precursor of the nitroxide did only displace small amounts of TA from what was expected to be the signal out of the thylakoid interior. The first experiment [30] imposes some – though rather wide – limits to TA enrichments in thylakoids, precision being small because the actual internal volume is only about 5% of the total, with a required correction for membrane volume of the same order of magnitude. The second experiment [31] assumes a specific binding of amines and is not pertinent to enrichments due, e.g., to donnan potentials or hydrophobic interaction. From the data presented here it is clear that at the measuring conditions used the donnan effect is small (comparison of volume data obtained with TA and TN by permeabilisation of chromium oxalate), but hydrophobic interaction with the membrane surface plays a major role.

The volumes derived for our preparation are at the lower limit of literature data obtained with different methods of 3–10 μl/mg Chl [52–57], which is in agreement with expectations for high osmolarity and high ionic strength, whereas the figures inferred from the total TA signal (sometimes more than 20 μl/mg Chl) would be quite 'far off'.

The calibration of the flash-induced signals leads to values for the internal buffering capacity higher than those obtained with neutral red, which amount to about 10 neq per mg Chl. [9] but volume data have not been assessed directly in that report). It has been shown that osmotic shrinkage leads to a concentration of buffer groups [9]. Considering this, the values for permeabilized preparations are approximately in agreement, and the crude approximation ($\beta_{int} \approx 100$ mM, i.e., $\approx$ 100 neq per mg) given here for more native preparations seems also reasonable, since a further increase of buffering is expected.

The comparison of the data also corroborates the conclusion [58] that membrane properties do not explain the differences in the effect of hydrophilic buffers between different preparations: the decay times of flash-induced signals were in both types of the order of 20 s (not shown). The lack of effect of buffers is not due to an exceptionally high internal buffering capacity. While this points to unusual properties of the internal phase, we have to reconsider ideas about structured water inside thylakoids: the rotational correlation times in the aqueous internal phase could not be determined very precise here but are certainly smaller than was assumed previously [31]. The deviation from values in free water can easily be accounted for by assuming a concentrated protein solution (made up from side chains of membrane-associated proteins, see [59]) in the interior. On the

other hand, probably most of the water resides in the hydration spheres of these proteins. We are dealing with rotational correlation times here rather than translational motility, which may indeed be lowered. Considering the low volumes found and the presence of high amounts of peptide side chains protruding into it, any model assuming a phase to be treated as free water in some sort of continuous compartment may be quite inadequate (see Refs. 60–62 for some ideas pertinent to this question). Especially free equilibration of concentration gradients in this compartment with localized buffer groups may be hampered (see the arguments for a similar effect in the partition region [63–65]).

The observed apparent increase in hindrance of rotation due to ΔpH [39] may be due to some shift in populations caused by internal acidification. With the small ΔpH values handled here, this difficulty is not expected to bias the calibration severely, though there may be small changes in spectral shape even here [12]. The H^+/e^--values obtained are not precise enough to pinpoint stoichiometries but do indicate that the internal volume of the organelle equilibrates with a considerable fraction and probably all of the protons translocated. They are underestimated due to some nonfunctional or nonthylakoid membranes in the preparation. ΔpH values produced by single flashes are in fair agreement with the data obtained from neutral red measurements.

A resolution of the fast kinetics is not feasible with the DTA-technique, but intermediate (20 ms) responses can be distinguished from faster ones. Generally speaking, this method to monitor proton deposition inside thylakoids produces results comparable with those obtained with neutral red but for the pronounced slow responses seen in absence of FeCy. These data are similar to results from one laboratory with chloroplasts under isoosmotic conditions [48] using the neutral red technique.

The most striking property of the slow responses is their sensitivity to uncouplers. A tentative explanation for several features of these phases, yet possibly only accounting for part of them can be offered by attributing them to an additional compartment undergoing alkalisation on flashes and a rather quick (several hundred ms) back reaction. Superimposing this on the transient seen with FeCy would produce an apparent slow rise like the one seen in the data and the fitting procedure cannot decide between this model and a third phase.

This explanation is favoured because in part of the preparations the spectrum of the response was different from the faster phases, indicating a heterogeneity of the spin population responding and because it explains easily the effect of uncouplers by invoking different compartments (simulations not shown).

The absence of slow phases with FeCy is understandable if the compartment in question is accessible to FeCy, leading to a suppression of the additional transients. The volume in question is, however, not affected by addition of up to 100 mM of zwitterionic buffers, so a low permeability of these buffers or a high local buffering capacity has to be postulated.

An obvious candidate for such an additional compartment would be a population of spins 'swimming' in the surface in the partition region of the grana, which has indeed been shown to slow spreading of concentration changes [63–65]. The effect of LA can then be understood as some destacking leading to enhanced signals (lowered buffering by surface groups), followed by a decrease of signal due to complete unstacking, entry of buffers and acceleration of proton diffusion.

There are some indications of a Q-cycle working under the measuring conditions used here [66,67]. It seems, however, that it can only produce a minor contribution to the slow responses particularly because proton translocation due to Q-cycles is expected to show pronounced oscillations with a period 2 in dark-adapted samples, which could not be demonstrated here.

The response seen in this study is a delocalized one, i.e., we cannot rule out localized gradients [68], whereas it seems as though under the experimental conditions studied here intramembrane spaces do not play a quantitatively predominant role (see Ref. 69 for a review on this subject). An important finding is the reproducibility of the dependence of buffer permeability on thylakoid preparation [58] with a different technique: the distribution method used here is at the worst slightly biased by binding the probe and so the

effect cannot only reflect an artifact caused by binding of neutral red [68].

The results concerning the additional signal seen in deactivated PS II-enriched preparations need further study, preferentially with another experimental technique. The absence of response with TTA excludes a simple surface phenomenon, whereas the stimulation of this response by alkaline deactivation of PS II and the pH-dependence argue against an association with normal proton transport. Furthermore, the decay of the main component of this response is 1–2 orders of magnitude slower than the decay of local alkalization due to hindrance of proton diffusion in the partition of grana stacks [65].

There is an indication of a reaction with similar kinetic characteristics seen with electrochromic absorption (reaction III of Ref. 7), but this response thought to represent a conformational change was not associated by the authors with inactivated material.

Appendix

Symbols. a, concentration of unprotonated amine; ah, protonated amine; V', ratio internal to external volume; β', ratio of buffering capacities [9]; K, dissociation constant; I, height of ESR-signal, first derivative peak to peak; ΔW, width, first derivative peak to peak; N, photosynthetic unit (see Methods); C, concentration of chlorophyll.

Indices. i, internal; b, external; t, total; Q, in presence of chromium oxalate.

From mass action $K = a \cdot h/ah$ it may be derived assuming

$$h_i = h_e = h, \quad a_i = a_e = a, \quad \text{and } da_i = da_e \tag{A-1}$$

$$dh_i = \frac{da_{ti}}{a_{ti}}(K+h)\frac{(1+V')}{(1+\beta'V')} \quad \text{(see Ref. 12)} \tag{A-2}$$

this can be related to ESR-signals, assuming a constant lineshape with $da_{ti}/a_{ti} = d(I_Q)/I_Q \cdot r$, r describing the nonlinearity of the function $I_Q = f(a_t)$ and obtained empirically (1.2–1.3 at 1 mM TA, 1.45–1.73 at 2 mM, and 2.16–3.3 at 4 mM Tempamine determined from the total internal signal). Total protons translocated, using the definition of the differential buffering capacity [9] $n_p = V_i\ dh_{it} = \beta_i\ dh_i V_i/h \ln 10$, total electrons $n_e = V_t C/N$, and $p := n_p/n_e$

$$p = \frac{NV'}{C}\frac{\beta_i}{\ln 10} r \frac{(K+h)}{h}\frac{dI_Q}{I_Q}\frac{(1+V')}{(1+\beta'V')} \tag{A-3}$$

the assumption $h_i = gh_e$ treated in a similar way to account for a 'dark ΔpH', i.e., a donnan potential or similar phenomenon leads with the reasonable assumption of $a_{ti} \approx a_{te}$ (for pH ≈ 7.5) to $g(1+V'g)/(1+\beta'V'g)$ instead of the last term.

V' is obtained from

$$V' = (I_Q W_Q^2)/IW^2 \tag{A-4}$$

If we take into account a factor (g_1) for the enrichment of a given nitroxide we get

$$V'_{app} = g_1 V' \tag{A-5}$$

To account for the enrichment of tempamine in the membrane surface (see Ref. 71 for a different treatment of the same phenomenon) we define an observable population (the index m referring to the membrane or membrane surface):

$$a_{to} = a_i + ah_i + ah_{mi} + ah_{me} + a_m \tag{A-6}$$

$$a_{te} = a_e + ah_e \tag{A-7}$$

All the concentrations of (A-6) are referred to internal aqueous volume such that

$$da_{to}V' = da_{te} \tag{A-8}$$

We insert distribution coefficients:

$$K_{i,e} = \frac{ah_{m\,i,e}}{ah_{i,e}} \quad \text{and} \quad K_m = \frac{a_m}{a} \tag{A-9}$$

and find

$$a_{to} = a_i + K_m a_i + \frac{(a_i h_i)(1+K_i+K_e)}{K}$$

$$:= a_i\left[1 + k_m + \frac{h_i g''}{K}\right]$$

$$\frac{a_{to}}{a_{te}} = g' = \frac{K}{K+h_e}\left[(1+K_m) + \frac{h_i g''}{K}\right] \approx 1 + g'' \tag{A-10}$$

$$da_{to} - da_{te} = \frac{K+h_i}{K} g'\, da_i - \frac{K+h_e}{K} da_e + \frac{a_i}{K} g''\, dh_i$$

$$- \frac{a_e}{K} dh_e$$

with $h_e = h_i$, $da_i = da_e$, $a_i = a_e$, $dh_i V'\beta' = -dh_e$, and Eqn. A-8:

$$da_{to} - da_{te} = (g' - 1)\, da_{te} + \frac{a_e}{K}(g'' + \beta' V')\, dh_i \qquad \text{(A-11)}$$

and with

$$da_e = \frac{K}{k + h_e} da_{te} - \frac{K a_{te}}{(K + h)^2} dh_e$$

and rearranging

$$da_{to}(1 + g'V') = \frac{a_{te}}{K + h}(g'' + g'\beta' V')\, dh_i \qquad \text{(A-12)}$$

and with $g' a_{te} = a_{to}$ and $g' \gg 1$, thus $g'' \approx g'$

$$dh_i = \frac{da_{to}}{a_{to}}(K + h)\frac{(1 + g'V')}{(1 + \beta' V')} \qquad \text{(A-13)}$$

again, $h_i = g h_e$ leads to

$$dh_i = g\frac{da_{to}}{a_{to}}(K + h)\frac{(1 + g'V')}{(1 + g\beta' V')} \qquad \text{(A-14)}$$

K_m, $K_{i,e}$ can be related to the data of Cafiso and Hubell by inserting estimates of the membrane volume [71], but here the use of g and g' as empirical factors is sufficient.

Experimentally, g is the enrichment of TA in the aqueous internal volume, g_1 the error in volume estimation by amine accumulation and g_2 is the enhancement (in the internal volume) due to cation enrichment of the buffering power of a buffer molecule present at an external concentration leading to a nominal capacity of β^*.

By definition

$$p = \beta_i / \ln 10 \cdot p_b \qquad \text{(A-15)}$$

experimentally accessible:

$$p_{b\,app} = \frac{N}{C} r \frac{(K + h)}{h} V'_{app} \frac{dI_Q}{I_Q} \qquad \text{(A-16)}$$

and for permeable buffers we find with $(1 + V') \approx (1 + \beta' V') \approx 1$

$$\frac{1}{p_b} = \frac{\beta_{int}}{p \ln 10} + \frac{\beta_{TA} + \beta_b}{p \ln 10} \qquad \text{(A-17)}$$

and

$$\frac{1}{p_{b\,app}} = \frac{g\beta_{int}}{g_1 p \ln 10} + \frac{g g_2 \beta^* b}{g_1 p \ln 10} \qquad \text{(A-18)}$$

it follows

$$p_{app} = \frac{g_1 p}{g g_2} \qquad \text{(A-19)}$$

and

$$\beta_{int\,app} = \frac{\beta_{int}}{g_2} \qquad \text{(A-20)}$$

for impermeable buffers and $\beta_b \approx \beta_{int}$: $\beta' V' \ll 1$ and

$$\beta_{int} = \left(\frac{p_{b\,app}}{p_{b\,app^b}} - 1\right)\frac{\beta_b}{gV'} + g_2 \beta^*_{TA} \qquad \text{(A-21)}$$

$p_{b\,app^b}$ measured in presence of impermeable buffer, hence

$$\beta_{int} = \frac{g}{g_1 \beta_{int\,app}}$$

and, with Eqn. A-15,

$$p = p_{app} \qquad \text{(A-22)}$$

Acknowledgements

Financial support of the Studienstiftung des Deutschen Volkes is gratefully acknowledged. I owe thanks to Prof. Dr. H. Metzner for support and encouragement, Prof. Dr. E. Bayer and Prof. Dr. H. Stegmann who kindly allowed the use of the ESR instrumentation, and Prof. Dr. H. Ninnemann who provided the HR 8-amplifier. I wish to thank Prof. Dr. K. Scheffler and Dr. H. Siefermann-Harms for fruitful discussions. P. Schuler provided expert help especially with the data acquisition.

References

1 Hangarter, R.P. and Good, N.E. (1982) Biochim. Biophys. Acta 681, 397–404.
2 Haraux, F. and De Kouchkovsky, Y. (1983) Physiol. Végét. 21, 563–576.

3 Westerhoff, H.V., Melandri, B.A., Venturoli, G., Azzone, G.F. and Kell, D.B. (1984) Biochim. Biophys. Acta 768, 252–292.
4 Slater, E.C., Barden, J.A. and Herweigh, M.A. (1985) Biochim. Biophys. Acta 811, 217–231.
5 Ferguson, S.J. (1985) Biochim. Biophys. Acta 811, 47–95.
6 Kell, D.B. (1986) Methods Enzymol. 127, 538–557.
7 Ausländer, W. and Junge, W. (1975) FEBS Lett. 59, 310–315.
8 Hope, A.B. and Morland, A. (1979) Aust. J. Plant Physiol. 6, 289–304.
9 Junge, W., Ausländer, W., McGreer, A.J. and Runge, T. (1979) Biochim. Biophys. Acta 546, 121–141.
10 De Wolf, F.A., Groen, B.H., Van Houten, L.P.A., Peters, F.A.L.J., Krab, K. and Kraayenhof, R. (1985) Biochim. Biophys. Acta 809, 204–214.
11 Junge, W., Schönknecht, G. and Förster, V. (1986) Biochim. Biophys. Acta 852, 93–99.
12 Wille, B. and Lavergne, J. (1982) Photobiochem. Photobiophys. 4, 132–144.
13 Rosen, G.M. (1974) J. med. Chem. 17, 358–360.
14 Sane, N., Yoshida, M., Hirata, H. and Kagawa, Y. (1977) J. Biochem. 81, 519–524.
15 Johnsson, S.M., Bangham, A.D. and Korn, D.E. (1971) Biochim. Biophys. Acta 233, 820–826.
16 Barenholz, Y., Amselem, S. and Lichtenberg, D. (1979) FEBS Lett. 210–214.
17 Reeves, J. and Dowber, R.M. (1969) J. Cell Physiol. 3, 47–60.
18 Keith, A.D., Snipes, W. and Chapman, D. (1977) Biochemistry 16, 634–641.
19 Arnon, D.J. (1949) Plant physiol. 24, 1–15.
20 Nakatani, H.Y. and Barber, J. (1977) Biochim. Biophys. Acta 461, 510–512.
21 Lilley, R. McC., Fitzgerald, M.P., Reenitz, K.G. and Walker, D.A. (1975) New Phytol. 75, 1–10.
22 Karlstam, B. and Albertsson, P.-Å. (1970) Biochim. Biophys. Acta 216, 220–222.
23 Ford, R.C. and Evans, M.C.W. (1983) FEBS Lett. 160, 159–164.
24 Boska, M.K., Blough, N.V. and Sauer, K. (1985) Biochim. Biophys. Acta 808, 132–138.
25 Dunahay, T.G., Staehelin, L.A., Seibert, M., Ogilvie, P.D. and Berg, S.P. (1984) Biochim. Biophys. Acta 764, 179–193.
26 Berthold, D.A., Babcock, G.T. and Yocum, C.F. (1981) FEBS Lett. 134, 231–234.
27 Berg, S.P. and Nesbitt, D.M. (1979) Biochim. Biophys. Acta 548, 608–615.
28 Bevington, P.R. (1969) Data Reduction and Error Analysis for the Physical Sciences, McGraw-Hill, New York.
29 Jentsch, W. (1969) Digitale Simulation kontinuierlicher Systeme, Oldenbourg, München.
30 Berg, S.P., Lusczakoski, D.M. and Morse, II, P.D. (1979) Arch. Biochem. Biophys. 194, 138–149.
31 Berg, S.P. and Nesbitt, D.M. (1982) Biochim. Biophys. Acta 679, 169–174.
32 Quintanilha, A.T. and Mehlhorn, R.J. (1978) FEBS Lett. 91, 104–108.
33 Keith, A.D., Bulfield, G. and Snipes, W. (1970) Biophys. J. 10, 618–629.
34 Bales, B.L. (1982) J. Magn. Res. 48, 418–430.
35 Windle, J.J. (1981) J. Magn. Res. 45, 432–439.
36 Vassermann, A.M., Kuznetsov, A.N., Kovarskii, A.L. and Bulachenko, A.L. (1971) Zh. Strukt. Khim. 12, 609–616.
37 Hall, J.E., Yodyanoy, I., Balasubramanian, T.M. and Marshall, G.M. (1984) Biophys. J. 45, 233–247.
38 Vistnes, A.J. and Puskin, J.S. (1981) Biochim. Biophys. Acta 644, 244–250.
39 Nesbitt, D.M. and Berg, S.P. (1980) Biochim. Biophys. Acta 593, 353–361.
40 Mulders, F., Van Langen, H., Van Ginkel, G. and Levine, Y.K. (1986) Biochim. Biophys. Acta 859, 209–218.
41 Mitchell, P. and Moyle, J. (1967) Biochem. J. 104, 585–600.
42 Walz, D., Goldstein, L. and Avron, M. (1974) Eur. J. Biochem. 47, 403–407.
43 Polya, G.M. and Jagendorf, A.T. (1969) Biochem. Biophys. Res. Com. 36, 696–703.
44 Golbeck, J.H., Martin, I.F. and Fowler, C.F. (1980) Plant Physiol. 65, 707–713.
45 Vernotte, C., Solid, C., Moya, I., Maison, B., Briantais, J.M., Arrio, B. and Johannin, G. (1983) Biochim. Biophys. Acta 725, 376–383.
46 Ausländer, W. and Junge, W. (1975) FEBS Lett. 59, 310–315.
47 Sandusky, P.O. and Yocum, C.F. (1986) Biochim. Biophys. Acta 849, 85–93.
48 Hope, A.B. and Matthews, D.B. (1984) Aust. J. Plant Physiol. 11, 267–276.
49 Vernotte, C., Solis, C., Moya, I., Maison, B., Birantais, J.M., Arrio, B. and Johannin, G. (1983) Biochim. Biophys. Acta 725, 376–383.
50 Etienne, A.L., Boussac, A. and Lavergne, J. (1981) in Photosynthesis (Akoyunoglou, G., ed.), Vol. II, pp. 405–413, Balaban International Sciences Servies, Philadelphia, PA.
51 Nordio, P.L. (1970) Chem. Phys. Lett. 6, 250–252.
52 Pasquirer, P. (1977) Thèse, Orsay, pp. 62ff.
53 Pfister, V.F. and Homann, P.H. (1986) Arch. Biochem. Biophys. 246, 525–530.
54 Rottenberg, H., Gunvald, T. and Avron, M. (1972) Eur. J. Biochem. 25, 54–63.
55 Heldt, H.W., Werdan, K., Milovancev, M. and Geller, G. (1973) Biochim. Biophys. Acta 314, 224–241.
56 Flores, S. and Graan, T. and Ort, D.R. (1983) Photobiochem. Photobiophys. 6, 293–304.
57 Dilley, R.A. and Rothstein, A. (1967) Biochim. Biophys. Acta 135, 427–443.
58 Hong, Y.Q. and Junge, W. (1983) Biochim. Biophys. Acta 722, 197–208.
59 Tiemann, R. and Witt, H.T. (1982) Biochim. Biophys. Acta 681, 202–211.
60 Van Kooten, O. (1984) TIBS 9, 221.
61 Sjöstrand, F.S. (1978) J. Ultrastruct. Res. 64, 217–245.
62 Srere, P.A. (1982) TIBS 7, 375–378.
63 Junge, W. and Polle, A. (1986) Biochim. Biophys. Acta 848, 265–275.

64 Junge, W. and McLaughlin, S. (1987) Biochim. Biophys. Acta 890, 1–5.
65 Polle, A. and Junge, W. (1986b) Biochim. Biophys. Acta 848, 274–278.
66 Velthuys, B.R. (1979) Proc. Natl. Acad. Sci. USA 75, 6081–6084.
67 Hangarter, R.P., Jones, R.W., Ort, D.R. and Witmarsh, J. (1987) Biochim. Biophys. Acta 890, 106–115.
68 Haraux, F. and De Kouchkovsky, Y. (1983) Phys. Végét. 21, 563–576.
69 Dilley, R.A., Theg, S.M., and Beard, W.A. (1987) Annu. Rev. Plant Physiol. 38, 347.
70 Vredenberg, W.J., Van Kooten, O. and Peters, R.L.A. (1984) in Advances in Photosynthesis Research (Sybesma, C., ed.), Vol. III, pp. 241–246, Martinus Nijhoff/Dr. W. Junk, Dordrecht.
71 Cafiso, D.S. and Hubbell, W.S. (1978) Biochemistry 17, 3871–3877.